ESA Contract Report

SMOS ESL contract 4000130567/20/I-BG

Contract Report to the European Space Agency

Annual SMOS brightness temperature monitoring report - 2021/22

Authors: Pete Weston and Patricia de Rosnay
Contract officer: Raffaele Crapolicchio

December 2022

Series: ECMWF - ESA Contract Report

A full list of ECMWF Publications can be found on our web site under:

http://www.ecmwf.int/publications/

European Centre for Medium Range Weather Forecasts
Shinfield Park, Reading, RG2 9AX, England

Abbreviations

BUFR .....Binary Universal Form for the Representation of meteorological data
CMEM .....Community Microwave Emissivity Modelling platform
ECMWF .....European Centre for Medium-range Weather Forecasts
ESA.....European Space Agency
IFS .....Integrated Forecast System
NRT .....Near Real Time
NWP .....Numerical Weather Prediction
RFI.....Radio Frequency Interference
SMAP .....Soil Moisture Active Passive
SMOS .....Soil Moisture and Ocean Salinity
Tb .....Brightness Temperature

1. Introduction

This document provides an annual summary of the performance of the European Space Agency (ESA) Soil Moisture and Ocean Salinity (SMOS) brightness temperature (Tb) monitoring run routinely at the European Centre for Medium-range Weather Forecasts (ECMWF). The period covered is September 2021 to August 2022. Several different monitoring plots are presented, and notable features are described in detail. Also, potential improvements to the monitoring system are proposed.

2. Annual SMOS monitoring results

Routine operational monitoring of SMOS observations from the NRT BUFR product is performed at ECMWF. The SMOS measured brightness temperatures are compared to short-term numerical weather prediction (NWP) forecasts transformed into brightness temperatures using the Community Microwave Emissivity Model (CMEM). The differences between these two quantities are known as background departures and statistics of these background departures are accumulated and plotted routinely.

The samples used to produce the plots can be filtered by area, including global, Northern and Southern Hemispheres, as well as loose definitions of the continents: Europe (120°W-120°E, 35°N-77.5°N), Asia (0°W-120°W, 40°N-82.5°N), North America (120°E-0°E, 20°N-77.5°N), South America (120°E-0°E, 40°S-17.5°N) and Australia (0°E-120°W, 47.5°S-7.5°S). This section focuses on global statistics.

Also, the plots are produced separately for data:

- Over sea or over land
- With different incidence angles: 30°, 40° or 50°
- With different polarisations: H (XX) or V (YY) at the SMOS antenna reference frame

A selection of different options for surface type, incidence angles and polarisations are presented, and the full set of plots are available via FTP at ftp://dpgswebserver-2.smos.eo.esa.int/SMOS_ESL2021/Task-5/Annual_Monitoring/2022/All_plots.zip).

A thorough introduction to the monitoring system can be found in Weston & de Rosnay (2022b) and examples of the plots produced can be seen at https://www.ecmwf.int/en/forecasts/quality-our-forecasts/monitoring/smos-monitoring. In this section each of the different types of plots produced as part of the SMOS monitoring system are presented and any notable features are highlighted to be investigated in more detail in the following sections.

2.1. Time series

Statistics are plotted as lines against time on the x-axis for the full twelve-month period with statistics accumulated in 12-hour chunks. The statistics plotted are mean and standard deviation of background departures, the mean observed and background brightness temperatures and number of observations. These plots allow global trends and jumps in the statistics to be identified.

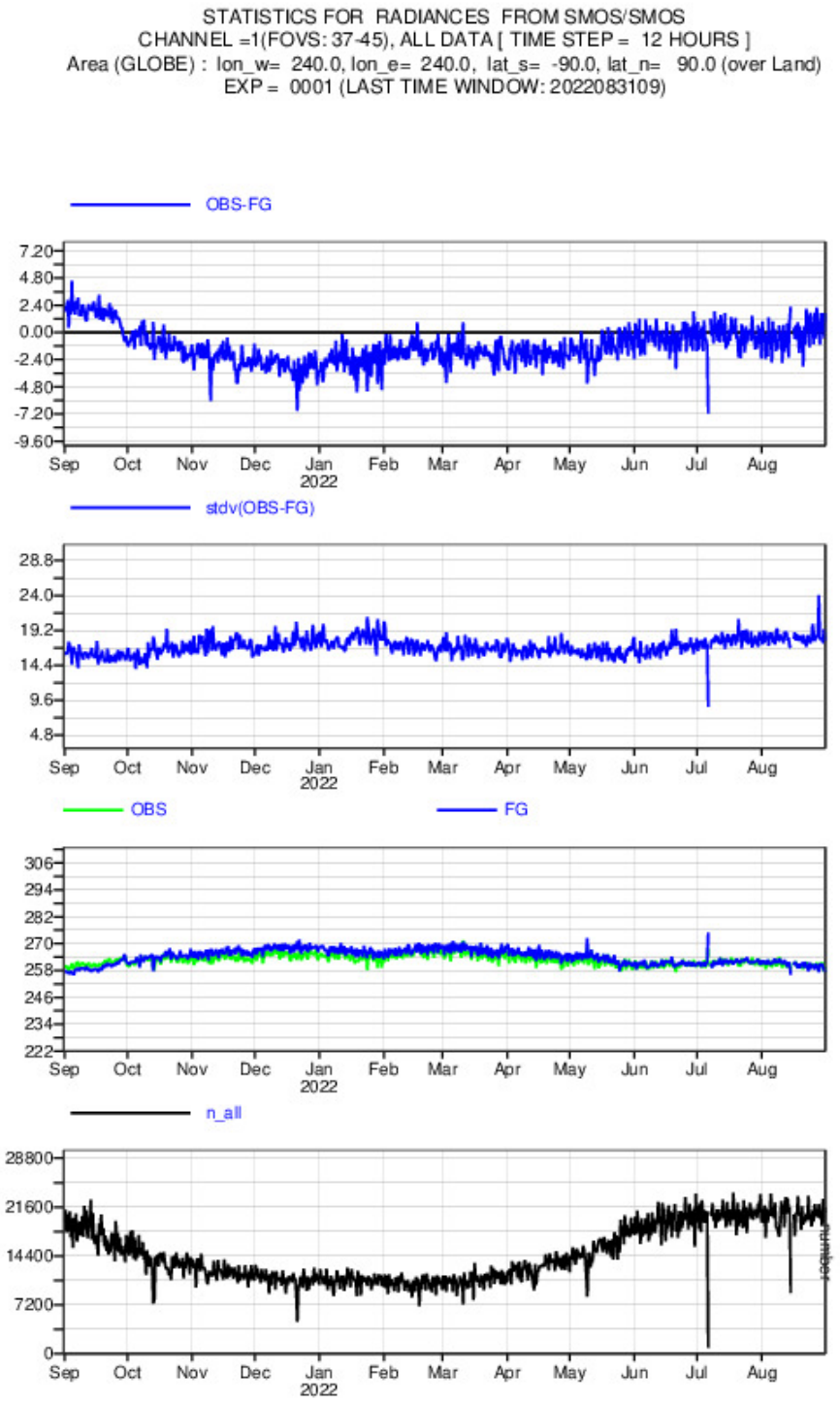

Figure 1: Time series of mean background departures (upper panel), standard deviation of background departures (2nd panel), mean observed and background values (3rd panel) and number of observations (lower panel). Statistics are accumulated into 12-hour bins for SMOS observations over land at 40° incidence angle, H polarisation and cover 1st September 2021 to 31st August 2022

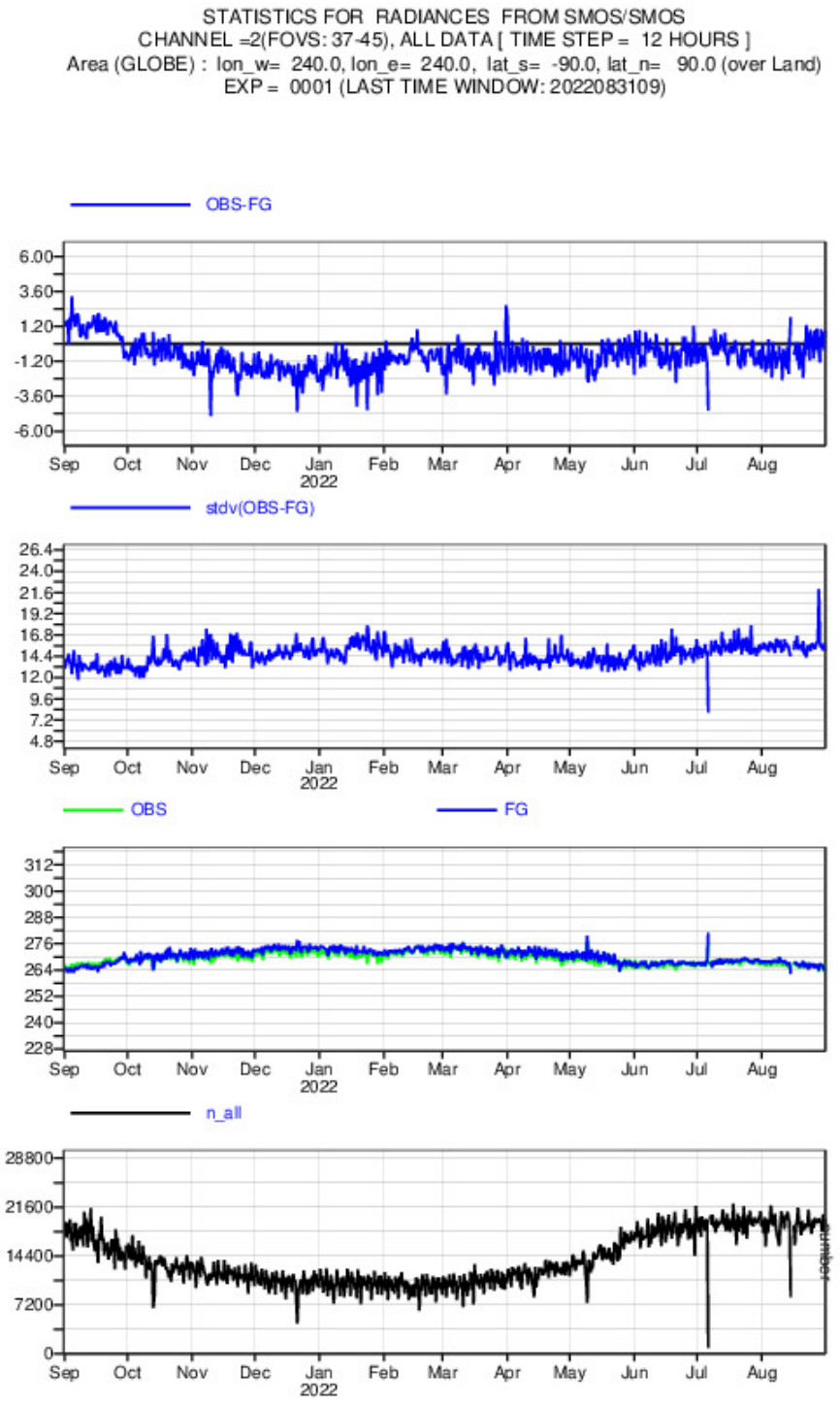

Figure 2: As figure 1 but for SMOS observations with V polarisation

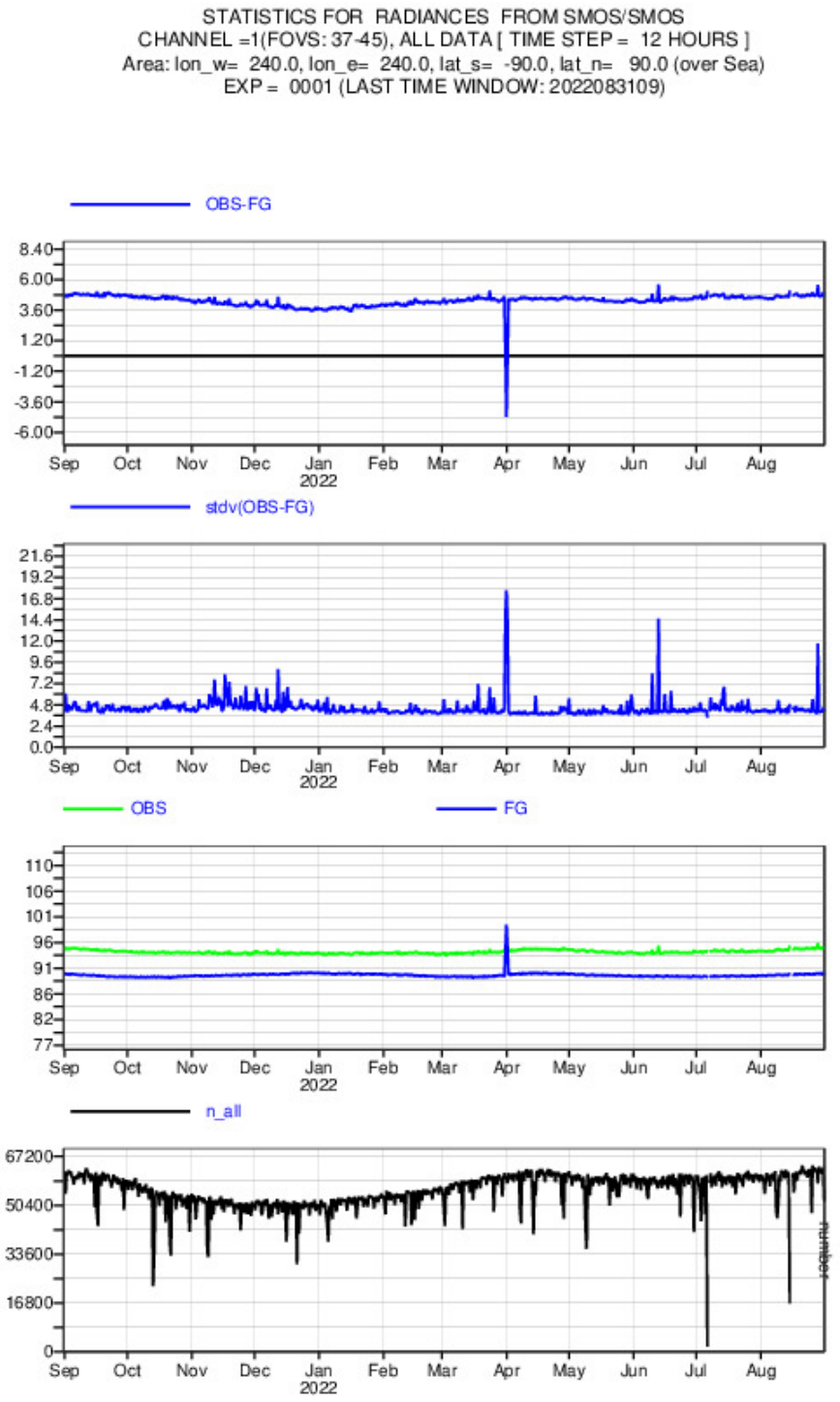

Figure 3: As figure 1 but statistics are accumulated for SMOS observations over ocean at 30° incidence angle, H polarisation and cover 1st September 2021 to 31st August 2022

Figures 1 and 2 show that the background departure statistics over land are generally very stable over the year. The mean background departures mostly vary between ±5K for H polarisations and ±3K for V polarisations with only very occasional global mean values outside of this range. The standard

deviation of background departures have slightly more day-to-day variability but generally stay close to a value of ~17K for H polarisations and ~14K for V polarisations. These values are smaller than the corresponding values from 2020/21 (Weston & de Rosnay, 2022a) due to the upgrade to v724 SMOS level 1 brightness temperatures in August 2021, with the associated enhanced RFI screening the main reason for this change. The apparent slightly better performance of the V polarisations over the H polarisations could be due to an instrument effect but it could also be due to differing performance of the CMEM observation operator used to convert the model soil moisture to brightness temperature. It should be noted that the first guess departures presented here do not have a bias correction applied and the statistics are consistent with those found between 2010 and 2016 without bias correction in de Rosnay et al (2020). See section 3.3 for some statistics before and after bias correction. The largest variation is seen in the number of observations monitored. Between September 2021 and December 2021 there is a significant reduction of almost 50% in the number of observations monitored. This is due to the Northern hemisphere winter and many observations over Northern hemisphere land surfaces being screened out due to frozen soil and snow. At the same time there is a corresponding negative shift in the mean background departures due to the different sampling as described in Weston & de Rosnay (2021). Between March 2022 and June 2022 this trend is reversed as the Northern hemisphere summer starts and the land thaws out.

Figure 3 shows that there is mostly less annual variability in the background departure statistics over ocean than over land. In previous years the variability over ocean was much larger due to sub-optimal sea-ice screening which was largely fixed with the quality control enhancements implemented on 11th May 2021. The number of observations between September 2021 and June 2022 is much more stable over ocean than over land due to smaller areas of ocean covered by sea-ice than snow-covered land areas. At the start of April there is a large spike in the mean and standard deviation of background departures. This was due to a period when the Faraday rotation angle was first missing and then incorrectly specified in the SMOS BUFR files. This then affected the calculation of the simulated brightness temperatures as shown in the third panel of figure 3. A detailed investigation into this issue can be found in section 3.1. There are also some smaller spikes in the departure statistics on the 13th June and 28th August 2022 which are related to potential instrument anomalies which are investigated in section 3.2.

2.2. Hovmöller plots

Statistics presented in this section are plotted as a heat map (Hovmöller plots) with time on the x-axis and latitude on the y- axis for the twelve-month period with statistics accumulated in 2.5° latitude bins and 12-hour chunks. The statistics plotted are mean and standard deviation of background departure, mean and standard deviation of observed value and number of observations. These plots allow local trends and jumps in the statistics to be identified.

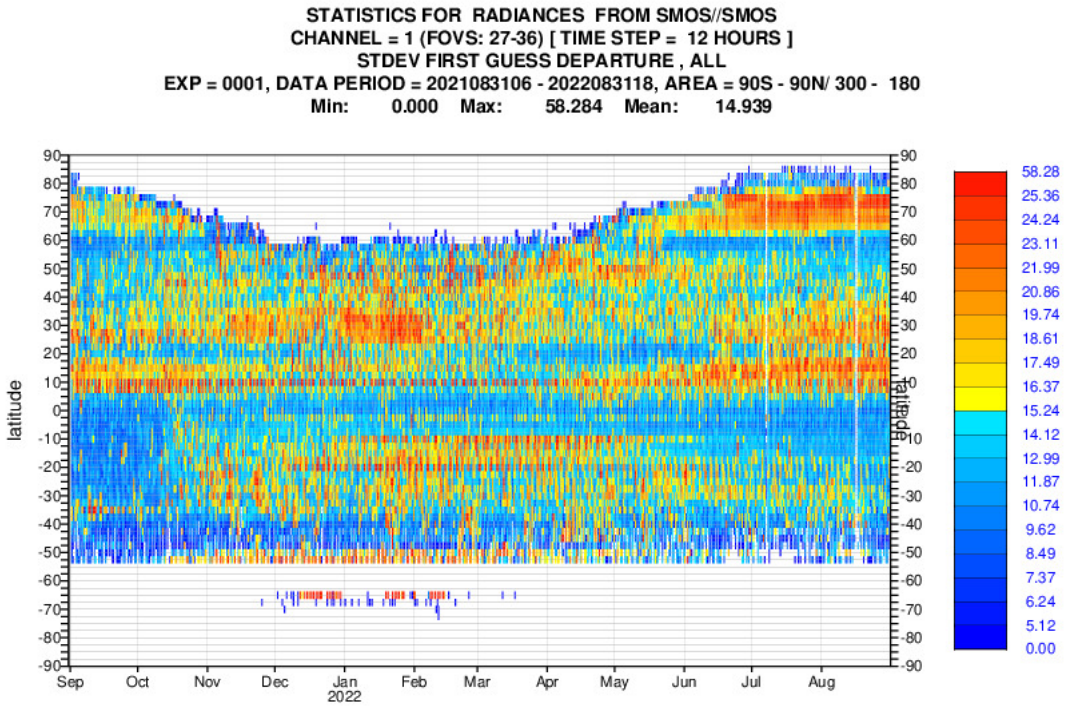

Figure 4: Hovmöller plot showing SMOS first guess departure standard deviation monitored over land at 30° incidence angle, H polarisation covering 1st September 2021 to 31st August 2022

Figure 4 shows various seasonal patterns in the variability of the background departures. In January there is an area of larger standard deviations of background departures around 30°N which is due to a new short-lived RFI source which was not fully screened out. There are also areas of larger standard deviations of background departures at 10-30°N in June, July, August and 10-30°S in December, January, February. These areas and times of year correspond to the wet season in the tropics and higher variability in model precipitation leading to higher variability in model soil moisture is the likely cause. Finally, there is also a large area of increased standard deviations of background departures between 60-80°N which corresponds to an area of positive bias in the background departures over Siberia. This is only visible in the Northern hemisphere (NH) summer because observations over these areas are screened out due to snow cover and frozen ground in NH winter, and can also be seen in the gridded maps in section 2.3.

In previous years such signals were masked by larger changes in the statistics due to RFI. With the improvements to the RFI screening in the v724 SMOS Tbs, the background departure statistics are now more sensitive to geophysical signals which is a significant step forward on the road to potential direct assimilation of the SMOS Tbs.

2.3. Maps

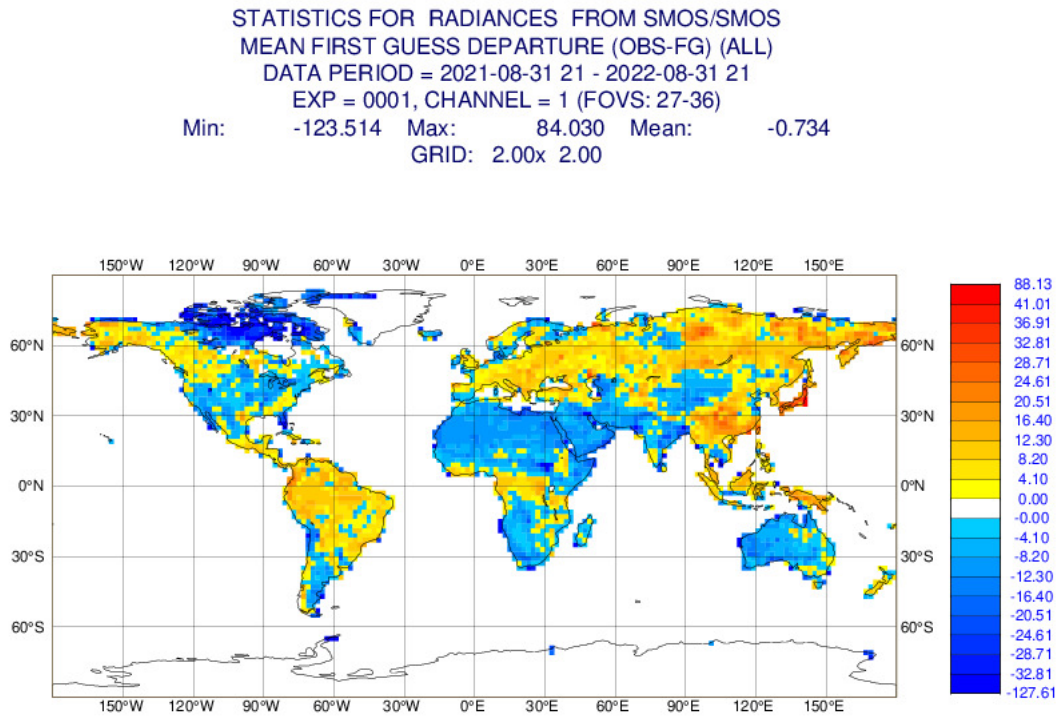

Figure 5: Gridded map plot showing the mean of SMOS background departures over land at 30° incidence angle, H polarisation covering 1st September 2021 to 31st August 2022

Figure 5 shows the geographical distribution of residual biases in the SMOS background departures. Although figures 1 and 2 show relatively small global mean background departures, figure 5 shows significantly large regional biases with large positive biases over Europe, Northern and Eastern Asia and South America; and large negative biases over large parts of Africa, South-Western Asia, Australia and the far North of North America. The distribution of biases has slightly changed since 2020/21 (Weston & de Rosnay, 2021) with some areas of previously positive biases over North America now screened out leading to a slight negative shift in the global bias as discussed in section 2.1. For more discussion on the sources of these biases see Weston & de Rosnay (2022c) and section 3.3 on the bias correction developments.

Figure 6 shows the largest variability in background departures remains over the Middle East, central and Eastern Asia, and to a lesser extent Europe. This is caused by RFI in those regions with the strength and location of RFI sources varying significantly throughout the year. The size of these signals is significantly reduced compared to previous years thanks to the improved v724 RFI screening although this map shows that the screening is still not perfect. However, other geophysical signals can start to be identified such as the higher variability over tropical Africa and Northern Australia relating to the tropical wet seasons as identified in figure 4.

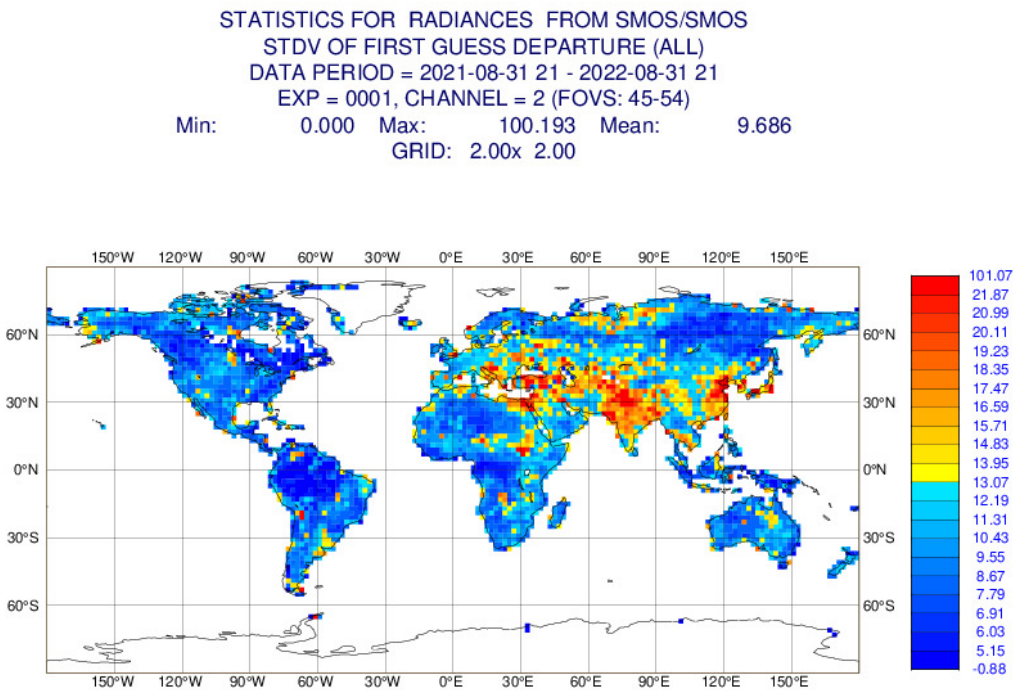

Figure 6: Gridded map plot showing the standard deviation of SMOS background departures over land at 50° incidence angle, V polarisation covering 1st September 2021 to 31st August 2022

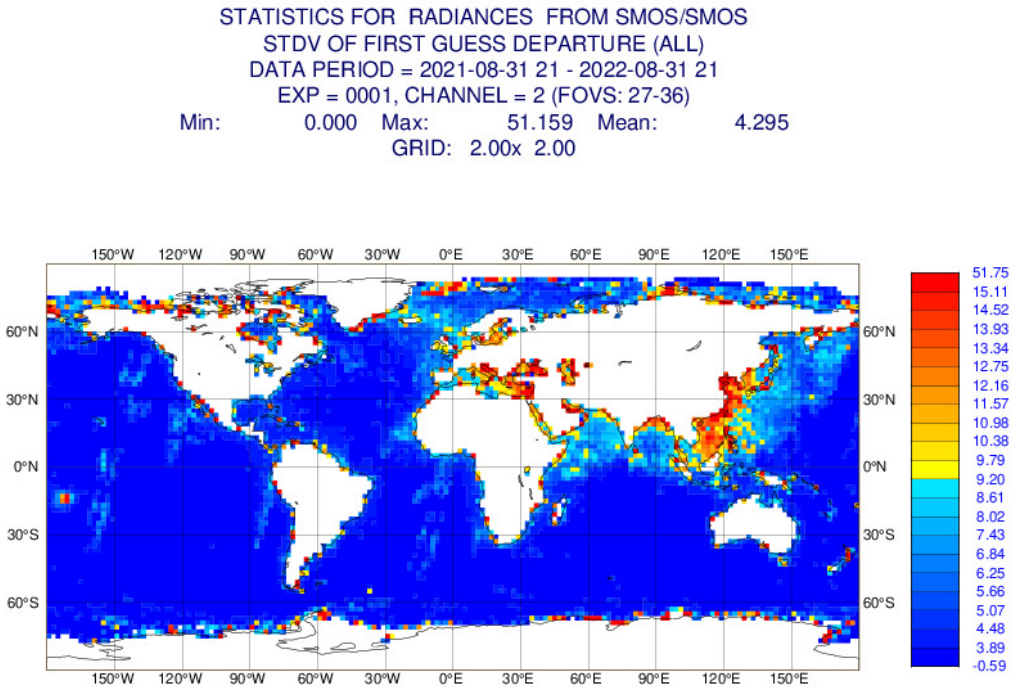

Figure 7: Gridded map plot showing the standard deviation of SMOS background departures over ocean at 30° incidence angle, V polarisation covering 1st September 2021 to 31st August 2022

Figure 7 shows areas of increased background departures surrounding the coasts of Europe and Asia due to RFI contamination. Over the Northern and Southern polar regions there are slightly increased background departures due to a combination of smaller sample sizes due to sea-ice screening and slight sub-optimalities in the sea-ice screening during rapid melting and freezing events. It should be noted the situation is much better than it was before 11th May 2021 when no model sea-ice information was used in the screening. Away from the RFI affected and polar regions there is very little variation in background departures due to lower Tb variations over ocean which are mostly caused by temperature variations. In addition, the observation operator CMEM treats the sea surfaces like lake surfaces. Hence, there is currently no variation in simulated brightness temperature from waves or surface wind-speed as there will be in the observed brightness temperatures.

2.4. Scatter

Statistics are accumulated from 1st September 2021 to 31st August 2022 and plotted as a 2-dimensional histogram with incidence angle on the x-axis and background departure on the y-axis. These plots allow the distributions of background departures at different incidence angles to be analysed.

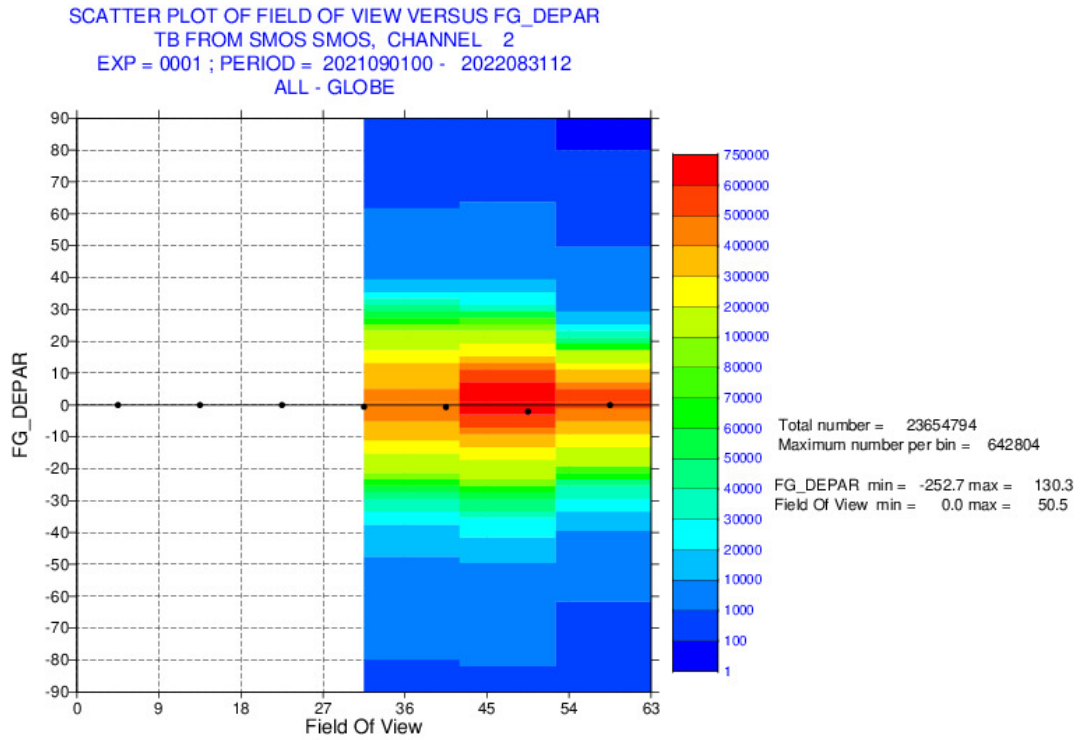

Figure 8: Scatter plot showing a 2D-histogram of SMOS background departures over land for different incidence angle bins, V polarization covering 1st September 2021 to 31st August 2022. The black dots represent the mean background departure for each incidence angle bin

Figure 8 shows that the distribution of background departures is centred close to zero for all incidence angle bins. It also shows that the histograms are close to symmetric, which can be seen by looking at the number of observations in the background departure bins with a similar magnitude but opposite

signs. The distributions of background departures are slightly narrower than in 2020/21 as seen by comparing figure 8 to figure 12 of Weston & de Rosnay (2022a). This is mainly due to the improved RFI screening since the implementation of the v724 L1c Tbs. The global mean background departures for each incidence angle bin are also close to zero although there are significant regional biases, see sections 2.3 and 3.3.

3. Notable features in 2021/22

This section describes notable features which are visible in the monitoring plots for September 2021 to August 2022.

3.1. Missing and incorrect Faraday rotation angle around 31st March/ 1st April 2022

Figure 9 shows that there was a period of larger negatively biased and larger standard deviations of SMOS background departures between 15:00 on 31st March 2022 and 16:00 on 1st April 2022. Just before this there was a period where the SMOS BUFR files were missing the Faraday rotation angle value which is usually specified with every SMOS observation location. This value is used at ECMWF as part of the simulation of model equivalent Tbs when the output Tb from CMEM is converted from the Earth frame of reference to the antenna frame of reference.

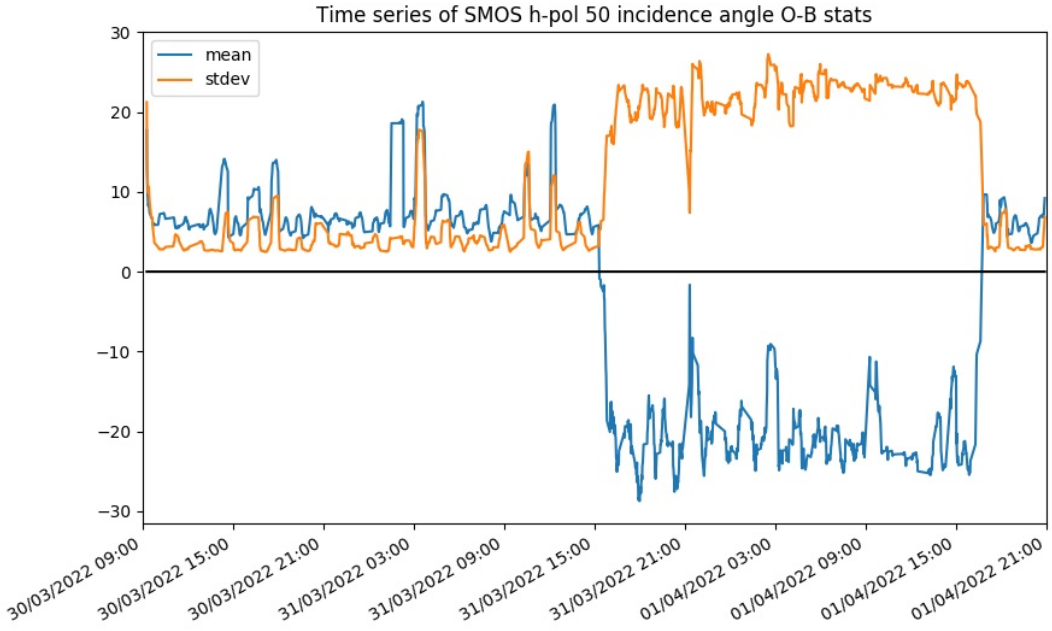

Figure 9: Time series of SMOS background departure statistics in one-minute bins for SMOS observations over ocean at 50° incidence angle, H polarisation between 09:00 on 30th March 2022 and 21:00 on 1st April 2022

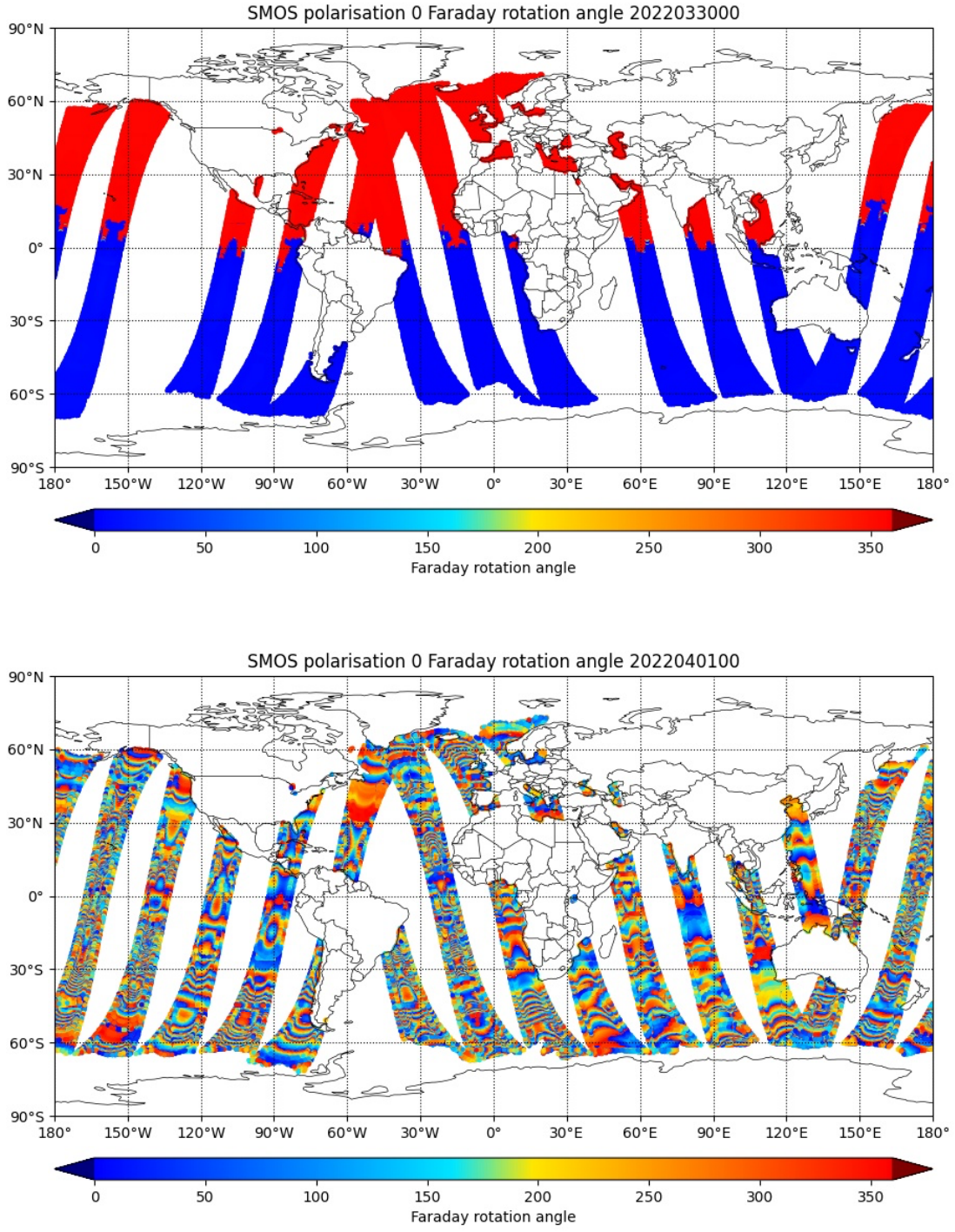

Figure 10: Snapshot maps showing SMOS Faraday rotation angles over ocean from 21:00 UTC on 29th March 2022 to 09:00 UTC on 30th March 2022 in the upper panel (representing normal values) and from 21:00 UTC on 31st March 2022 to 09:00 on 1st April 2022 in the lower panel (representing the incorrect values)

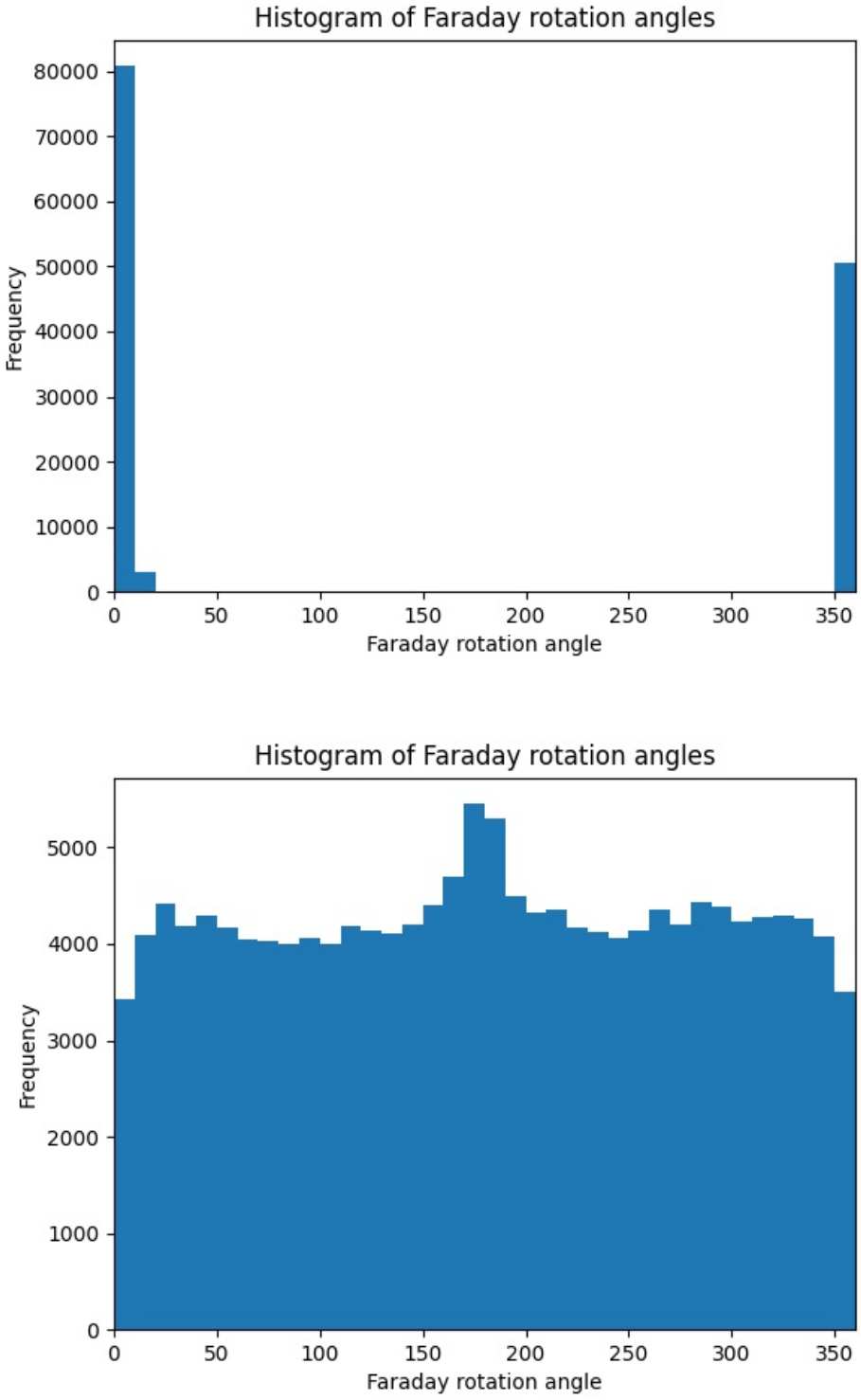

Figure 11: Histograms of Faraday rotation angles over ocean from 21:00 UTC on 29th March 2022 to 09:00 UTC on 30th March 2022 in the upper panel (representing normal values) and from 21:00 UTC on 31st March 2022 to 09:00 on 1st April 2022 in the lower panel (representing the incorrect values)

Normally the Faraday rotation angle value is close to 0 or 360 degrees, see upper panels of figures 10 and 11, so a missing value (assumed to be 0) actually doesn't cause large differences in the simulated model equivalent Tbs. The Faraday rotation angle was missing between 01:00 and 15:00 on 31st March 2022. However, between 15:00 on 31st March 2022 and 16:00 on 1st April 2022, exactly coinciding with the anomalous background departures, the Faraday rotation angles were provided from a climatological file and these values appear to have been corrupted as they varied almost uniformly between 0 and 360 degrees, see lower panels of figures 10 and 11. ESA is investigating this issue. Once the nominal Faraday rotation angles returned at 16:00 on 1st April 2022 the SMOS background departure statistics return to their nominal values. Therefore, it is clear that the cause of the degraded background departures was the usage of the Faraday rotation angles from the climatological file.

3.2. Potential instrument anomalies on 13th June and 28th August 2022

On the 13th June and 28th August there were spikes in the standard deviation of background departures over ocean as seen in figure 3. Figure 12 shows the time series of background departure statistics from these events have very similar signatures, a large increase in both the mean and standard deviation of background departures. For the 13th June this happened between 03:53 and 04:26 and for the 28th August this happened between 17:46 and 18:28.

Figure 13 shows the background departure maps for both cases with the 13th June event affecting observations over the central Pacific Ocean and the 28th August affecting the South-Eastern Atlantic Ocean. It is the observed Tbs which show the large differences during the anomalies compared to the times either side while the simulated Tbs are consistent throughout suggesting both were instrument anomalies. Figure 13 shows that, during the anomaly, the majority of observed Tbs are significantly warmer than the simulated Tbs by up to 100K.

Figure 12 shows H polarisation observations while figure 13 shows V polarisation observations so this indicates that both polarisations were similarly affected. There were no anomalies highlighted in the relevant SMOS weekly reports, but the 13th June anomaly did coincide with a solar radio burst (https://www.spaceweatherlive.com/en/archive/2022/06/13/xray.html) which is the most likely explanation.

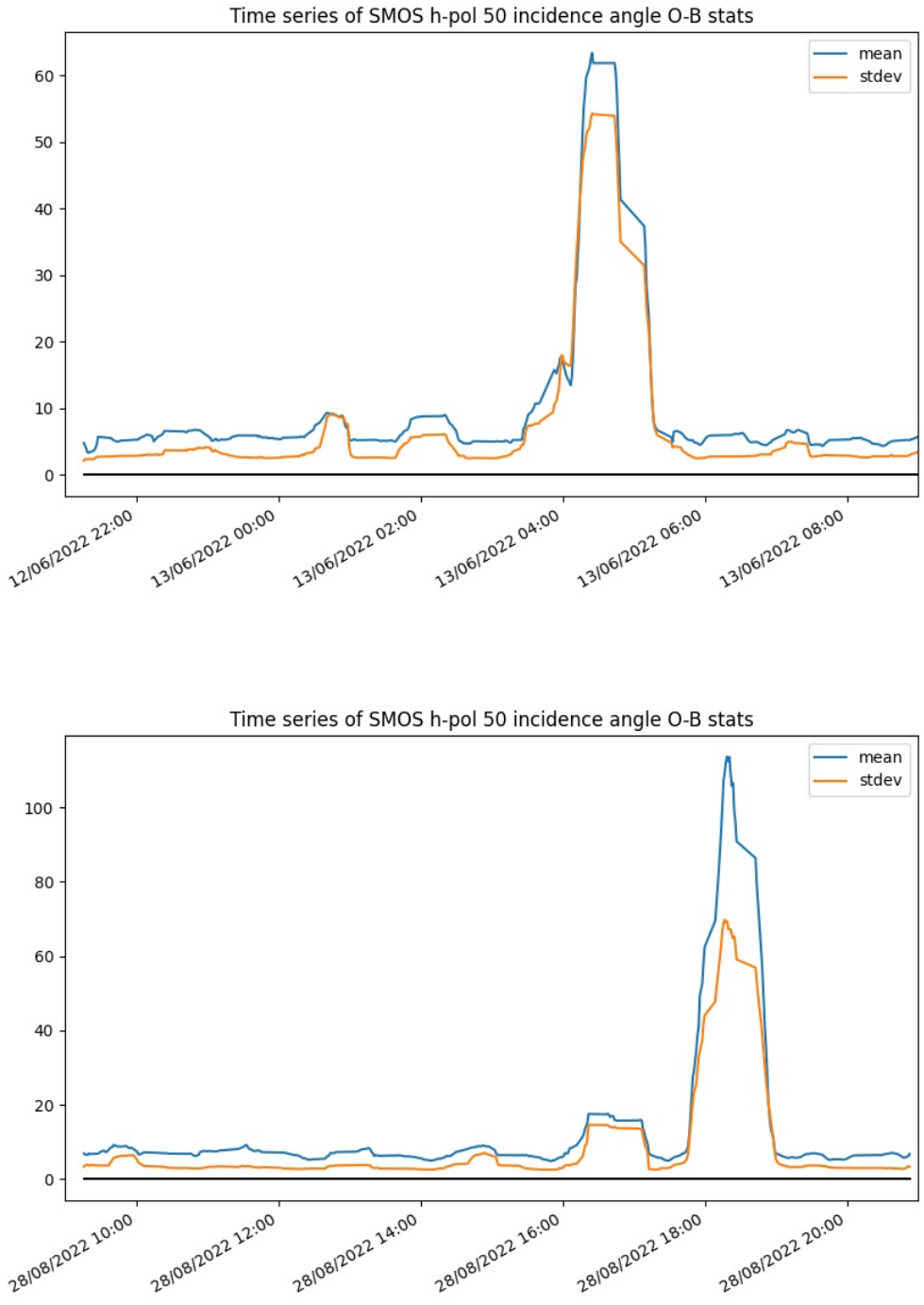

Figure 12: Time series of SMOS background departure statistics in one-minute bins for SMOS observations over ocean at 50° incidence angle, H polarisation between 21:00 on 12th June 2022 and 09:00 on 13th June 2022 (upper panel) and between 09:00 and 21:00 on 28th August 2022 (lower panel)

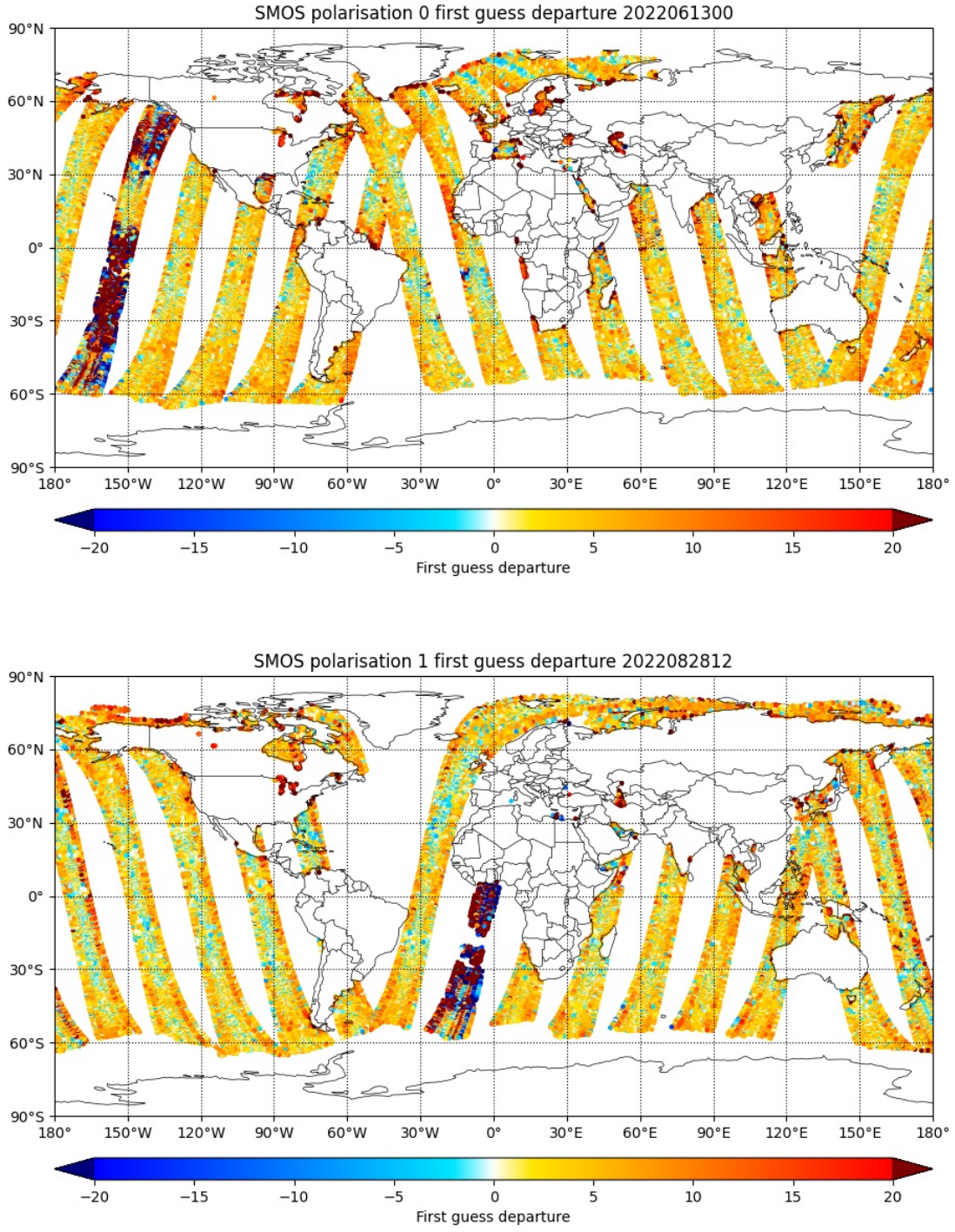

Figure 13: Snapshot maps showing SMOS background departures at V polarisation over ocean from 21:00 UTC on 12th June 2022 to 09:00 UTC on 13th June 2022 (upper panel) and from 09:00 UTC to 21:00 UTC on 28th August 2022 (lower panel)

3.3. Bias correction

As part of a multi-year SMOS monitoring project, a new bias correction has been developed for SMOS Tbs against the ECMWF simulated model equivalents coming from the ERA5 reanalysis. This uses a cumulative distribution function (CDF) matching approach with geographical and seasonal variations in order to correct the regional biases as seen in figure 5 and seasonally varying biases as seen in figure 1 and 2. For more details of the method see Weston & de Rosnay (2022c).

It is planned to use this bias correction in future direct SMOS Tb assimilation experiments so the performance of the bias correction based on ERA5 data needs to be assessed against recent operational data. Here, the bias correction (trained on data between 2014 and 2017) is applied to a year of SMOS Tb data between September 2021 and August 2022.

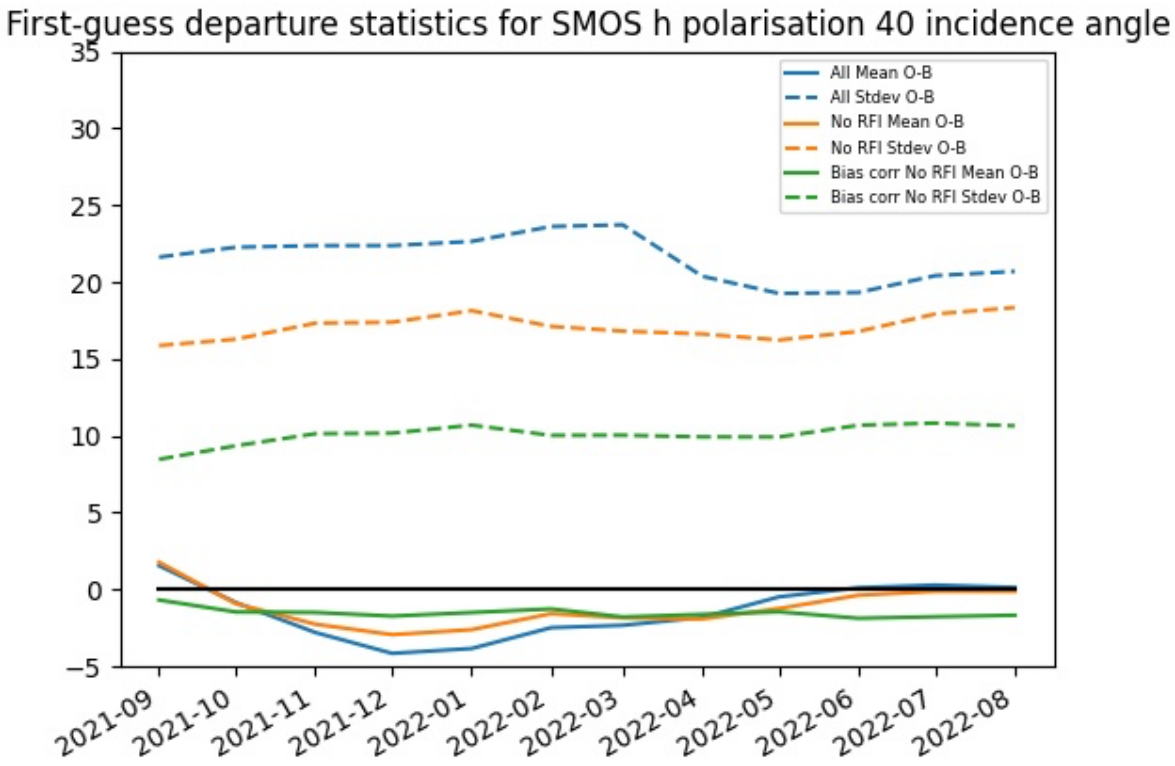

Figure 14: Time series of mean background departures (solid lines) and standard deviation of background departures (dashed lines) for all data (blue), RFI screened data (orange) and bias corrected data (green). Statistics are accumulated into 12-hour bins for SMOS observations over land at 40° incidence angle, H polarisation and cover 1st September 2021 to 31st August 2022

Figure 14 shows that the seasonal variations in bias are almost completely removed in the mean background departures after bias correction. However, the global residual biases are slightly negative at ~-1-2K which is a larger absolute residual than that shown in Weston & de Rosnay (2022c). The bias correction also results in a significant reduction in the standard deviation of background departures from

values of ~16-17K after RFI screening to ~9-10K after bias correction. This is a slightly smaller albeit comparable reduction to that shown in Weston & de Rosnay (2022c).

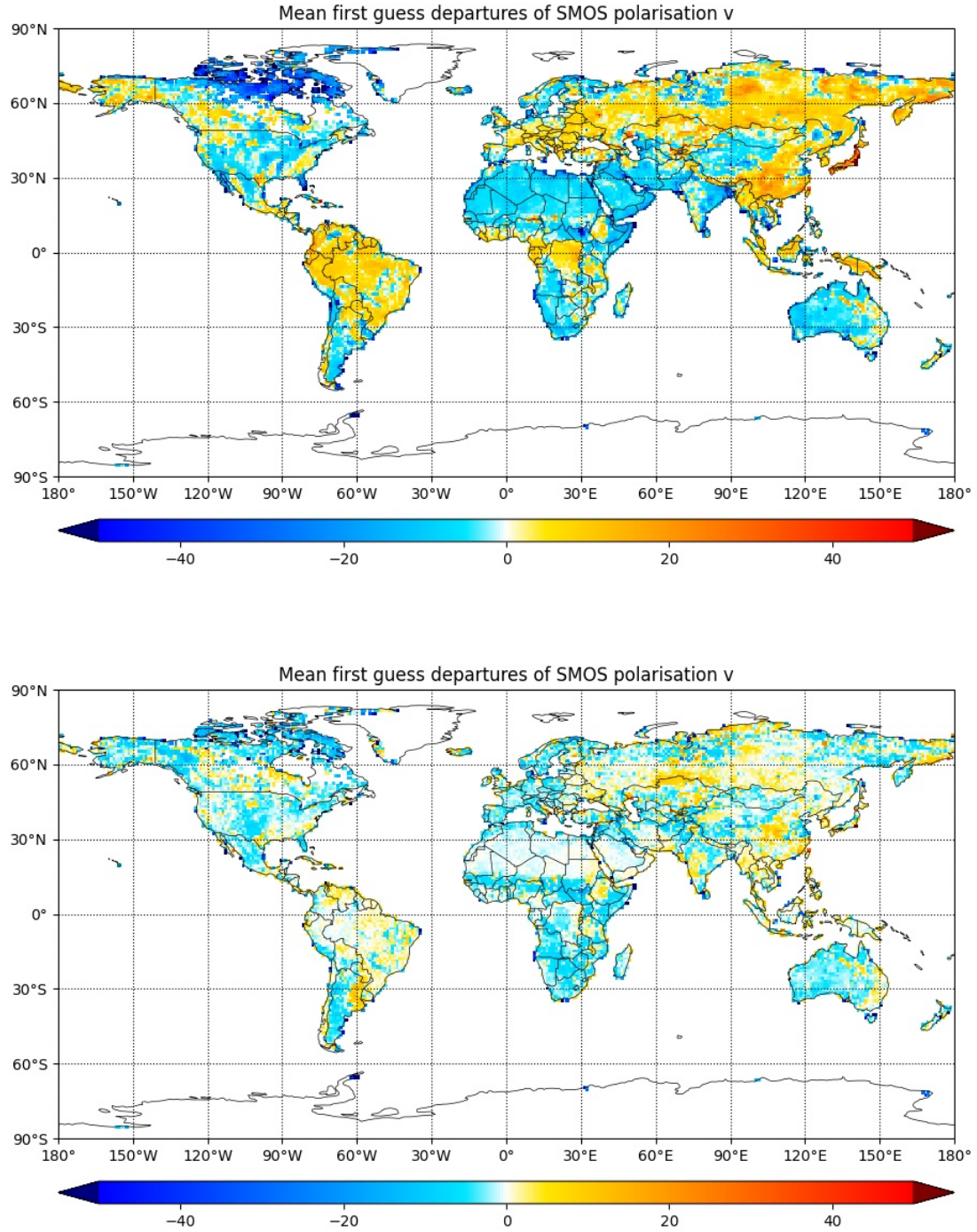

Figure 15: Gridded map plot showing the mean of SMOS background departures over land before bias correction (upper panel) and after bias correction (lower panel) at 40° incidence angle, V polarisation covering 1st September 2021 to 31st August 2022

Figure 15 shows that the regional biases are significantly reduced over the whole globe with the best performance over the arid regions of the Sahara and Middle East. Elsewhere there are still some residual biases although these are much smaller after bias correction than they were before bias correction, as expected.

Overall, the bias correction is performing fairly well when tested on recent SMOS background departures statistics, although the global performance is not quite as strong as illustrated in Weston & de Rosnay (2022c). This is to be expected due to changes in the model climatology between the cycle used for ERA5, 41r2, implemented operationally in March 2016, and the current model cycle, 47r3, implemented operationally in October 2021. This is an inherent problem with using historical data to train such a CDF-matching approach. See section 4.1 for potential enhancements to the bias correction approach.

4. Future enhancements to the monitoring system

4.1. Bias correction

Section 3.3 describes the newly developed bias correction and preliminary offline results when applying this bias correction to SMOS data from 2021/22. A possible enhancement would be to apply this to the SMOS data being processed through the operational monitoring within the IFS. Work is underway to do this in the context of testing the direct assimilation of SMOS Tbs so this should be implemented within the next couple of years.

In section 3.3, a drawback of the current approach, using historical data to calculate the CDF-matching parameters, was highlighted. There is ongoing work to enhance this approach by using an adaptive bias correction for other soil moisture observations assimilated into the simplified extended Kalman filter (SEKF) land assimilation system. The aim is to update the CDF-matching parameters on a day-to-day basis, thus responding to changes in bias more dynamically. Applying this approach to the SMOS Tbs could be investigated in the future to improve on the results shown in section 3.3 and will be relevant for future assimilation experiments too.

4.2. Improved monitoring over ocean

There is ongoing work at ECMWF to improve the sea-ice and coastal screening in other MW radiance observations which could be applied to SMOS data in the future. In particular, the use of FASTEM (Liu et al., 2011) as part of the RTTOV (Saunders et al., 2018) radiative transfer model to calculate surface emissivities over ocean could be used to produce more realistic and accurate simulated Tbs for SMOS over ocean. In coastal areas a weighted average of the FASTEM/RTTOV simulated Tb and the CMEM simulated Tb using the fraction land-ocean mask information could be used. This has the potential to significantly improve the quality of the background departures in coastal regions and could lead to the relaxation of the coastal screening documented in section 3.1.

4.3. Observation operator enhancements

As discussed in section 3.3, sub-optimalities in the observation operator are one of the potential sources of the residual biases in the SMOS background departures. As part of a new Horizon Europe project called CERISE (CopErnIcus Climate change Service Evolution), starting in January 2023, there will be

work to enhance the observation operator for low frequency microwave observations in general (including at L-band frequencies) using machine learning approaches. This will hopefully lead to improved performance leading to smaller biases in the SMOS background departures in the future. The timescale on this project is that the newly developed observation operator should be available in 2025.

5. Comparisons to SMAP

Since 11th May 2021 the monitoring of the NASA Soil Moisture Active Passive (SMAP) instrument has also been part of the ECMWF operational system, using the same framework as the SMOS monitoring. SMAP was launched in 2015 and the instrument measures at L-band (1.41GHz) the same frequency as SMOS and therefore comparisons between the monitoring statistics for SMOS and SMAP are very relevant for unpicking observation and model issues in the background departures.

The comparisons presented in section 5.1 were made with data from September 2021 to August 2022 with the v724 SMOS L1 Tbs and most up-to-date SMAP Tbs in the operational system. The SMOS observations used in the comparison are limited to those with incidence angles between 39.5° and 40.5° which best match the 40° incidence angles of the SMAP observations. Also, the operational screening including the most up-to-date RFI screening is applied to the SMOS data. By contrast, SMAP has onboard RFI screening which is applied to the data before it arrives at ECMWF. CMEM with the same settings is used as the observation operator or both the SMOS and SMAP observations.

5.1. September 2021 to August 2022 comparison

Figure 19 shows that the standard deviation of background departures is slightly smaller for SMAP than for SMOS for V polarisation. The SMAP mean background departures are more negatively biased with the magnitude of bias larger than for SMOS. Despite these small differences between SMOS and SMAP, the statistics are largely comparable and the results agree with comparisons made previously (Weston & de Rosnay, 2022a). At the most recent end of the time series, from late July 2022 onwards, the statistics for SMAP are missing and this coincides with a period where the SMAP instrument was put into “safe mode” meaning that no scientific data was measured. In early October the SMAP data returned allowing SMAP Tb monitoring at ECMWF to continue and comparisons between SMOS and SMAP will continue to be made.

Figure 20 shows that the gridded standard deviation of background departures are significantly smaller for SMAP than they are for SMOS with the largest differences in Asia, the middle East and South-Eastern Europe, all areas where there are significant RFI sources. This indicates that the onboard screening for SMAP is still doing a better job than the v724 SMOS screening. In addition, over areas not affected by RFI, the SMAP standard deviation of background departures are also smaller than for SMOS albeit to a slightly lesser degree. This indicates that SMAP has lower instrument noise than SMOS which is expected because the SMOS instrument was designed to reduce the noise by averaging over different incidence angles. In this analysis only a small range of SMOS incidence angles are used so there is no reduction in noise from the use of multiple incidence angles.

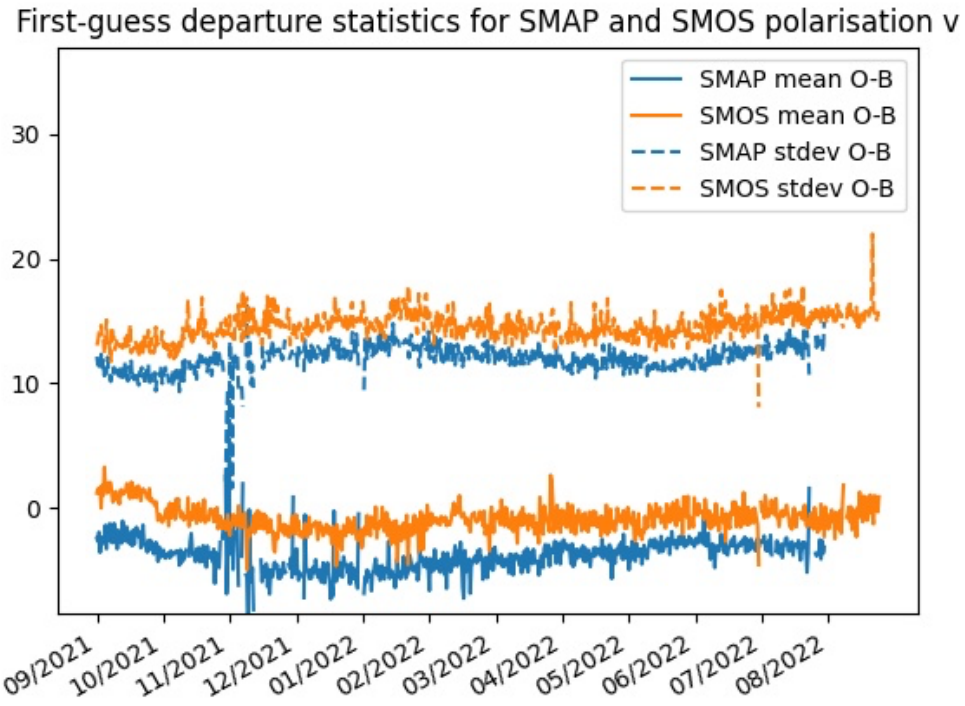

Figure 19: Time series of mean (solid lines) and standard deviation (dashed lines) of background departures for SMAP (blue) and SMOS (orange) for V polarisation between 1st September 2021 and 31st August 2022

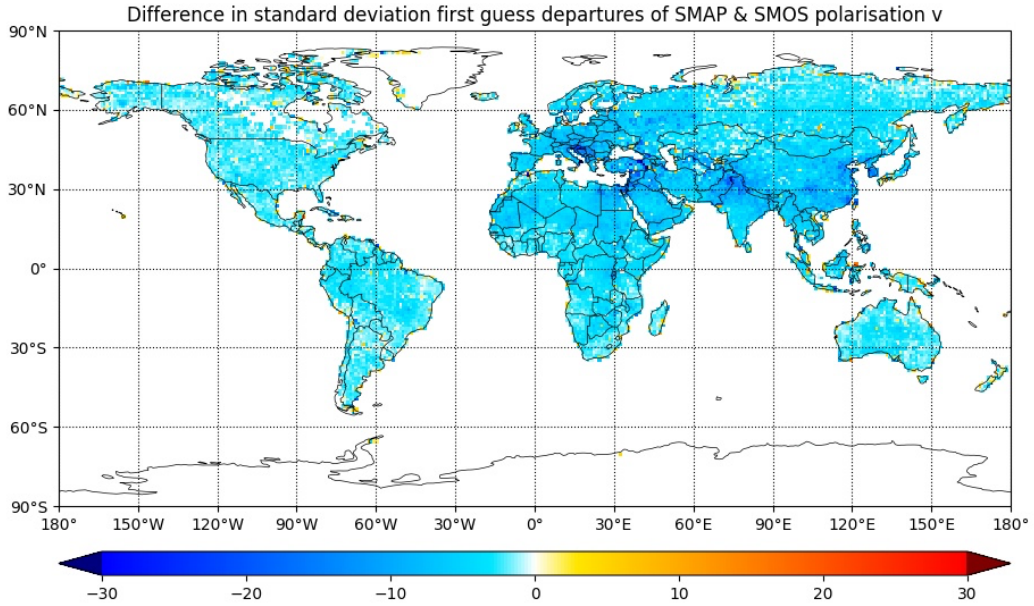

Figure 20: Difference in gridded standard deviation of background departures for V polarisation between SMAP and SMOS. Statistics are calculated between 1st September 2021 and 31st August 2022

References

de Rosnay, P., J. Muñoz-Sabater, C. Albergel, L. Isaksen, S. English, M. Drusch, J.-P. Wigneron: SMOS brightness temperature forward modelling and long term monitoring at ECMWF. Remote Sens. Environ., 237 (2020): 111424. https://doi.org/10.1016/j.rse.2019.111424

Liu, Q., Weng, F., and English, S.: An improved fast microwave water emissivity model, IEEE, T. Geosci. Remote, 49, 1238–1250, 2011.

Saunders, R., Hocking, J., Turner, E., Rayer, P., Rundle, D., Brunel, P., Vidot, J., Roquet, P., Matricardi, M., Geer, A., Bormann, N., and Lupu, C.: An update on the RTTOV fast radiative transfer model (currently at version 12), Geosci. Model Dev., 11, 2717–2737, https://doi.org/10.5194/gmd-11-2717-2018, 2018.

Weston, P., P. de Rosnay: Annual SMOS brightness temperature monitoring report - 2019/20. ESA contract report. SMOS ESL contract 4000130567/20/I-BG, January 2021

Weston, P., P. de Rosnay: Annual SMOS brightness temperature monitoring report - 2020/21. ESA contract report. SMOS ESL contract 4000130567/20/I-BG, January 2022a

Weston, P., P. de Rosnay: Quality control plan for brightness temperature monitoring - 2022. ESA contract report. SMOS ESL contract 4000130567/20/I-BG, April 2022b

Weston, P., P. de Rosnay; Multi-year SMOS brightness temperature monitoring. ESA contract report. SMOS-E contract 4000125399/18/I-BG, July 2022c